Accurate Estimation of the Nonlinearity of Input/Output Response for Color Cameras

Vien Cheung,[1] Stephen Westland,[1,*] and Mitch Thomson[2]

[1]Centre for Colour Design Technology, School of Design, University of Leeds, Leeds LS2 9JT, UK

[2]Color & Imaging Institute, University of Derby, Derby, DE22 3HL UK

Received 18 March 2003; revised 23 February 2004; accepted 17 March 2004

Abstract: This study investigates techniques for accounting for the nonlinearity of the input/output response of a camera system. A simple power-law form of the nonlinearity was assumed and estimates of the value for the exponent for each of the color channels were made using three different methods. The responses from an Agfa StudioCam camera were linearized and then device characterization was attempted. Characterization errors were up to 10% better using the spectral-sensitivities-based method for estimating the nature of the nonlinearity than using the other two methods. We therefore suggest that the spectral-sensitivities-based method should be preferred for characterization or any other computational process that requires linearization of the camera responses. We expect greater benefits using this method for "low-end" camera systems and/or for cameras where the spectral sensitivities are known or more precisely estimated. We also expect the smoothness of the illumination to influence the error in the estimates of the nonlinearity using the luminance- and mean-reflectance-based methods. © 2004 Wiley Periodicals, Inc. Col Res Appl, 29, 406–412, 2004; Published online in Wiley InterScience (www.interscience.wiley.com). DOI 10.1002/col.20061

Key words: color reproduction; device characterization; input/output nonlinearity; gamma

INTRODUCTION

The need to be able to measure color properties of complex images and the proliferation of low-cost devices in the consumer market has led to increased interest in performing color measurement using digital color cameras. Several methods exist to enable colorimetric transformations between input-device *RGB* values and some device-independent space such as CIE *XYZ* values.[1–5] Such colorimetric transformations are often referred to as device characterization and involve two main processes.[6] First, camera sensor values (*RGB*) are obtained for targets with known color characteristics (that is, with known illuminant and reflectance spectra or with known CIE *XYZ* values). Second, these sensor values are transformed to match the known CIE values. This transformation is sometimes attempted using a linear transform. However, many color digital camera systems exhibit a nonlinearity (sometimes termed a tone-reproduction curve) between the input intensity and the output response of the color channels. Although the sensor (charge-coupled device or CCD in short) material gives a linear response to light intensity, a nonlinearity is often added by the camera manufacturer. Therefore a linearization process is highly desirable before attempting the linear transform. Even when the colorimetric transformation is achieved using a nonlinear transform it is beneficial to linearize the camera response values.[4]

Previous studies suggest a simple approach to linearization that uses luminance or mean spectral reflectance of a series of gray samples.[3,7] However, to estimate the nonlinearity robustly it is necessary to know the spectral sensitivities of each of the color channels.[8] The true input/output nonlinearity cannot be determined without at least a crude estimate of the channel spectral sensitivity profile, because the "input" in this case is the energy entering the sensor class in question. The relationship between the nonlinearity of the sensor response and the spectral sensitivity of a channel is inherent in the work of Barnard and Funt, who described methods to estimate the spectral sensitivities of

*Correspondence to: Professor Stephen Westland (e-mail: s.westland@leeds.ac.uk)

the channels of a camera system.[9] Indeed, Barnard and Funt demonstrated that when estimating the spectral sensitivities of the channels it was beneficial to jointly fit the linearization and the channel response functions.

This article explores the effectiveness of methods to estimate the input/output nonlinearity in the context of camera characterization. The work extends a previous study, which demonstrated that various techniques may be used to estimate the input/output nonlinearity for camera systems.[10] These techniques included methods based on the luminance and mean reflectance of a set of neutral samples and methods based on a knowledge (or estimation) of the spectral sensitivities of the channels and were evaluated using a computational model of a camera system. In that previous study[10] the significance of a proper estimation of the input/output nonlinearity was shown by comparing the accuracy of characterization using different linearization techniques with the camera model. In this study the analysis is extended for a real imaging system because it is known that the inevitable presence of noise in such systems can have a great effect on characterization procedures.[9,11]

BACKGROUND

Consider that a spatially uniform surface of known spectral reflectance $P(\lambda)$ is captured under an illuminant with known spectral power distribution $E(\lambda)$ by a three-channel imaging system with spectral sensitivities $S_R(\lambda)$, $S_G(\lambda)$, and $S_B(\lambda)$. Thus, if we represent the variables by discrete samples at uniform intervals of wavelength λ the raw channel responses R, G, and B for the red, green, and blue channels respectively are given by the following:

$$R = \Sigma E(\lambda) S_R(\lambda) P(\lambda)$$
$$G = \Sigma E(\lambda) S_G(\lambda) P(\lambda) \quad (1)$$
$$B = \Sigma E(\lambda) S_B(\lambda) P(\lambda).$$

We assume that the channels are subject to a nonlinearity f to generate the actual output responses R', G', and B'. Eq. (2) shows an example for the blue channel; similar nonlinearities are assumed to exist for red and green channels as follows:

$$B' = f(B). \quad (2)$$

Very often the nonlinearity can be modeled using a power-law function as follows:

$$B' = B^{\gamma}, \quad (3)$$

where the exponent γ may be set by the manufacturer to compensate for the nonlinear relationship between the digital input to a typical display device (e.g., CRT monitor) and the luminance output of such a display device. We note, however, that other authors have used different forms for the correction of the nonlinearity. Barnard and Funt, for example, compared a correction where the camera was considered linear apart from for the two extremes with a correction that was based on an exponential fit.[9] The exponent γ in Eq. (3) can be estimated, for the blue channel, from pairs of data (B, B') obtained from a small number of measurements. Recall, however, that to compute the raw channel input (B) the spectral sensitivity of the channel is required [Eq. (1)]. Nevertheless, the luminance Y is expressed as follows:

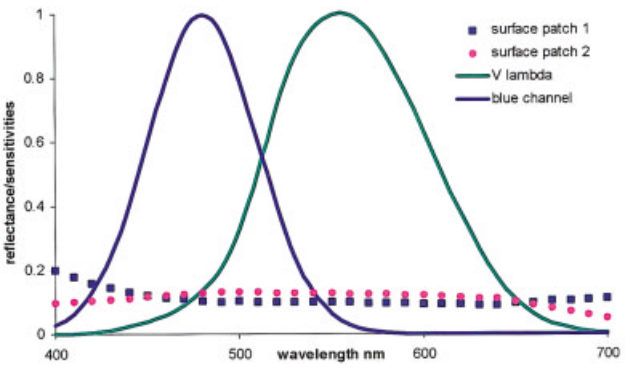

FIG. 1. Reflectance spectra of two hypothetical gray surfaces with spectral reflectance that varies with wavelength.

$$Y = \Sigma E(\lambda) V(\lambda) P(\lambda), \quad (4)$$

where $V(\lambda)$, the luminous efficiency function of each surface, is often used instead of the actual channel input B to determine the input/output nonlinearity function f.

Thus, an exponent γ is found according to a least-squares criteria fit for Eq. (5) as follows:

$$B' = Y^{\gamma}. \quad (5)$$

If the luminance is identical to (or a linear transform of) the actual channel input B of the system, the exponent estimated using the luminance values will be identical to the true value of the exponent that we would estimate if the values of B were known (with similar arguments for the other two channels).

In Fig. 1 the reflectance spectra of two hypothetical surfaces are shown with the spectral sensitivity of a blue channel and the luminous efficiency $V(\lambda)$ curve. Note that surface patch 2 has a reflectance that is consistently higher than that of surface patch 1 in the wavelength region that contributes to the $V(\lambda)$ response, whereas this is not the case in the region of the blue channel. Consequently, although the two surfaces shown in Fig. 1 would have different Y tristimulus values they would produce rather similar responses for the blue channel if viewed under an equal-energy illumination.

The extent to which the exponent estimated from Eq. (5) will be the same as that estimated from Eq. (3) depends partly on the degree to which the reflectance spectra of the samples used in the linearization process change with wavelength. For this reason that neutral samples are commonly used. However, we note that if the actual spectral sensitivities of the camera channels were known (so that the raw channel responses R, G, and B could be computed and Eq. (3) used), then colored samples could be used to estimate the nonlinearity of the channels.

ALGORITHM

Suppose the camera output values for a range of surfaces, defined by spectral reflectance factors $P(\lambda)$, are captured under an illumination, defined by spectral power distributions $E(\lambda)$, by a camera system of known channel spectral sensitivities $S_R(\lambda)$, $S_G(\lambda)$, and $S_B(\lambda)$ and nonlinear input/output response. Raw camera output values will then be given by Eq. (1).

The raw channel response for each surface/illuminant combination is assumed to be subject to a gamma-like input/output nonlinearity. Thus, the camera output values R', G' and B' are related to the raw camera outputs by a power law with exponent γ [Eq. (6)] as follows:

$$\begin{aligned} R' &= R^{\gamma} \\ G' &= G^{\gamma} \\ B' &= B^{\gamma}. \end{aligned} \tag{6}$$

Different techniques to estimate the nonlinearity of the channels are investigated in this article. These techniques include methods based on the luminance and mean reflectance of a set of neutral samples and methods based on a knowledge (or estimation) of the spectral sensitivities of the channels. For the case where the luminance or mean reflectance of the samples was used, the value of γ was estimated for Eqs. (7) and (8) respectively using linear algebra to perform a least-squares fit as follows:

$$\begin{aligned} R' &= Y^{\gamma} \\ G' &= Y^{\gamma} \\ B' &= Y^{\gamma} \end{aligned} \tag{7}$$

$$\begin{aligned} R' &= P^{\gamma} \\ G' &= P^{\gamma} \\ B' &= P^{\gamma}. \end{aligned} \tag{8}$$

For the case where the camera spectral sensitivities are known or estimated, the exponent was estimated based on Eq. (6).

A parametric model for the estimation of the channel response distributions has been suggested[8] in which the characteristics of the color channels are fitted with basis functions of the Gram–Charlier expansion[12] thusly:

$$R_\lambda \approx (1 + s_r\lambda + 2k_r\lambda^2)a_r \exp\left(-\left(\frac{\lambda-\lambda_r}{w_r}\right)^2\right). \tag{9}$$

In Eq. (9) each spectral response distribution is treated as possibly skewed, possibly kurtosed Gaussian functions. In total the model had five parameters: the peak wavelength λ_r, amplitude a_r, and width w_r of the Gaussian, together with the skewness s_r and kurtosis k_r terms. The values of these five parameters were determined for each of the color channels using a gradient-based optimization technique based on dynamic hill climbing.[13] We note that other methods exist in the literature for estimating the spectral sensitivities of the channels.[9,14,15] The focus of this article, however, is not the accurate estimation of the channel sensitivities and the method that we used is sufficient to generate crude approximations of these sensitivities.

The impact of any errors in the estimation of the nonlinearity was evaluated by performing a complete characterization of the camera system and inspecting the resultant errors in the $R'G'B' \rightarrow XYZ$ transform.

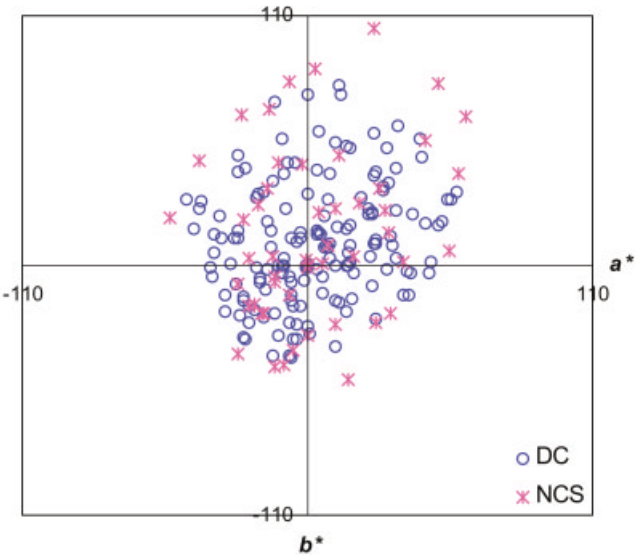

FIG. 2. Color distributions of 166 Macbeth ColorChecker DC (DC) and 50 NCS samples (NCS) in CIELAB a^*b^* diagram

EXPERIMENT

An Agfa digital StudioCam camera, a three-chip CCD device with 8-bit resolution for each channel and 4500 × 3648 pixel spatial resolution, was used in this study. During the experiment the automatic white-balance setting was disabled. Two imaging targets, 166 Macbeth ColorChecker DC (excluding the repeated gray-scale colors located around the boundary of the chart) and 50 Natural Color System (NCS) selected samples, were used for the characterization. The spectral reflectance factors of the patches on the two charts were measured using an X-Rite 938 spectrodensitometer. The color distributions of the selected ColorChecker DC and NCS samples are presented in the CIELAB a^*b^* diagram as shown in Fig. 2. A Minolta CS1000 spectroradiometer was used for the measurement of the spectral power distribution of the illuminating source. The lighting system consisted of two gas-filled tungsten lamps arranged approximately in a 45/0 illumination/viewing geometry.

CIE tristimulus values were computed for the patches using the 1964 CIE observer data and our measured illuminant data. A collection of the neutral Munsell surfaces (specifically N6/ to N9/ with 0.5 value interval) were used to determine the nature of the input/output nonlinearity using each of three techniques (luminance, mean reflectance, spectral sensitivities) detailed as follows.

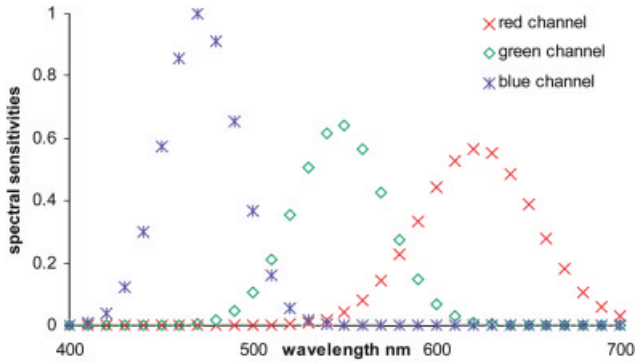

FIG. 3. Estimated channel spectral sensitivities.

Luminance- or mean-reflectance-based technique

1. Determine the value of the exponent for each channel to transform the luminance [Eq. (7)] or the mean reflectance [Eq. (8)] of the Munsell gray samples to the channel response.
2. Apply the estimates of the exponents to the measured camera responses for the DC samples to yield the linearized *RGB* values for those samples.
3. Perform spatial correction to minimize the effect of any spatial nonuniformity of the intensity of the illumination or of the sensitivity of the camera CCD.[7,16]
4. Compute the coefficients of a polynomial transform that maps *RGB*→ *XYZ* based on the *RGB* and *XYZ* values of the DC samples.
5. Compute the CIELAB color difference between the actual *XYZ* values and the *XYZ* values obtained from step 3 for the DC samples. We refer to the average CIELAB color difference for these samples as the training or memorization error.
6. Use the polynomial transform obtained from the DC samples to compute *XYZ* values for the NCS samples and compute CIELAB color differences between the actual and predicted values. We refer to the average CIELAB color difference for these samples as the testing or generalization error.

Spectral-sensitivities-based technique

1. Determine the value of the exponent for each channel to transform the Luminance [Eq. (7)] of the Munsell gray samples to the channel response.
2. Apply the estimates of the exponents to the measured camera responses for the DC samples to yield the linearized *RGB* values for those values.
3. Perform spatial correction to minimize the effect of any spatial nonuniformity of the intensity of the illumination or of the sensitivity of the camera CCD.[7,16]
4. Estimate the spectral sensitivities of the camera using the linearized *RGB* values of the DC samples (Fig. 3 shows the estimates that were obtained).
5. Use the estimates of the spectral sensitivities to re-estimate the values of the exponents using the Munsell gray samples and Eq. (6).
6. Apply the new estimates of the exponents to the measured camera responses for the DC samples to yield the linearized *RGB* values.
7. Compute the coefficients of a polynomial transform that maps *RGB*→ *XYZ* based on the *RGB* and *XYZ* values of the DC samples.
8. Compute the CIELAB color difference between the actual *XYZ* values and the *XYZ* values obtained from step 6 for the DC samples.
9. Use the polynomial transform obtained from the DC samples to compute *XYZ* values for the NCS samples and compute CIELAB color differences between the actual and predicted values.

Thus for each technique we attempt to obtain linearized camera responses and then use a polynomial to map these responses to the CIE tristimulus values. For the spectral-sensitivities-based techniques we require linearized values before we can begin to estimate the spectral sensitivities. Therefore a crude estimate of the nonlinearity is attempted (using the luminance-based-technique), the spectral sensitivities are estimated, and then the spectral sensitivities are used to re-estimate the nonlinearity (exponents). The procedure adopted used the DC samples to test the memorization performance of the characterization procedure and the NCS samples to test the generalization performance. That is, the polynomial transform was computed using the DC samples and tested using the DC (memorization) and NCS (generalization) samples. The polynomial was implemented by a 3×20 transform as follows:

$$\mathbf{T} = \mathbf{MC}, \tag{10}$$

which had been found to give best performance in some related studies[17,18] where $\mathbf{T}$ is an $n \times 3$ matrix of tristimulus values for n samples, $\mathbf{M}$ is an $n \times 20$ matrix of augmented linearized camera responses, and $\mathbf{C}$ is a 20×3 matrix of coefficients. Each row of $\mathbf{M}$ contained the following terms $[R\ G\ B\ RG\ RB\ GB\ R^2\ G^2\ B^2\ RGB\ R^2G\ G^2B\ B^2R\ R^2B\ G^2R\ B^2G\ R^3\ G^3\ B^3\ 1]$.

All computations were performed using MATLAB. The coefficients of the polynomials [Eq. (10)] were determined using pseudoinverse methods.[19]

RESULTS

Table I shows the values of the exponent that were estimated using each of the three linearization techniques.

TABLE I. Estimation of the exponent using each of the three different linearization techniques.

Linearization techniques	Estimate of exponent		
	Red channel	Green channel	Blue channel
Spectral sensitivities	1.3977	0.8507	1.3139
Luminance	1.4045	0.8527	1.3203
Mean reflectance	1.3774	0.8325	1.2948

TABLE II. Comparison of memorization and generalization performance (3 × 20 polynomial transform) with different linearization techniques.

	Memorization			Generalization		
	Spectral sensitivities	Luminance	Mean reflectance	Spectral sensitivities	Luminance	Mean reflectance
Median ΔE	1.3153	1.3937	1.4026	2.3325	2.5726	2.5931
Maximum ΔE	7.1643	7.4551	7.6585	14.3971	15.0397	15.3466

Table II shows the characterization performance for the DC and the NCS samples based on linearization by the various techniques. Because the $RGB \rightarrow XYZ$ transformation is not perfect, characterization errors will still be obtained even if the input/output nonlinearity is estimated perfectly.

In Table II the memorization performance is shown using each of the linearization techniques for the DC samples that were used to develop the polynomial characterization transform. Generally, the maximum ΔE is quite similar in all three cases but the median color difference is lowest for the case where linearization was performed using an estimate of the channel spectral sensitivities.

The generalization performance is shown for the NCS samples. The median ΔE for the case using the spectral-sensitivities-based linearization technique is 10% and 9% lower respectively than for the mean-reflectance- and luminance-based techniques. This study demonstrates that an accurate linearization that uses a crude estimate of the spectral sensitivities of the camera channels can reduce characterization errors by approximately 10% compared with traditional techniques.

To elaborate the reasons why the spectral-sensitivities-based technique enables better color characterization than the other two techniques, we attempted to find the best linear transform between the linearized camera responses and the tristimulus values for the DC samples. In so doing we inherently assume that the camera spectral sensitivities are a linear transform of the color-matching functions and accept that this is only likely to be approximately true. Thus, we find the coefficients a–i for Eq. (11) as follows:

$$\begin{aligned} X &= aR + bG + cB \\ Y &= dR + eG + fB \\ Z &= gR + hG + iB. \end{aligned} \tag{11}$$

Although the extent to which the camera responses may be subject to a linear transform to yield the tristimulus values depends on the relationship between the spectral sensitivities and the color-matching functions, we argue that the better the linearization technique the better such a linear transform [Eq. (11)] will be possible. Table III shows the characterization errors for the camera system using Eq. (11) and each of the three linearization techniques. It is evident that the characterization errors are smallest for the spectral-sensitivities-based technique.

Figure 4 shows plots of $(aR + bG + cB)$ against X, $(dR + eG + fB)$ against Y, and $(gR + hG + iB)$ against Z for each of the linearization techniques for both the DC samples (on the left) and the NCS samples (on the right). Note that the coefficients a–i were computed using the DC samples.

If the linearization technique is useful, then the points in Fig. 4 should fall on straight lines with gradient 1. The correlation coefficients r obtained by the ratio of the covariance of the values of the ordinate (y) and abscissa (x) divided by the product of the individual variances[20] were computed thusly:

$$r = \frac{S_{xy}}{S_x S_y}. \tag{12}$$

Table IV lists the correlation coefficients r for the plots shown in Fig. 3. Note that the r values are always closer to unity for the plots derived from the spectral-sensitivities-based linearization technique when compared with the equivalent plots derived from the other two techniques.

More interestingly, however, note that for the DC samples (which were used to derive the values a–i) the spectral-sensitivities-based technique always generates linear transforms that produce plots (Fig. 4) close to the ideal gradient, whereas this is not the case for the other two linearization techniques. In fact, the luminance-based technique performs well for the DC samples for the Y tristimulus value (middle left in Fig. 4) but not so well for the X tristimulus value (upper left in Fig. 4). This can be explained by the fact that the computation of luminance involves the $V(\lambda)$ function, which is also used to compute Y. We note that some au-

TABLE III. Comparison of memorization and generalization performance (3 × 3 linear transform) with different linearization techniques.

	Memorization			Generalization		
	Spectral sensitivities	Luminance	Mean reflectance	Spectral sensitivities	Luminance	Mean reflectance
Median ΔE	2.2510	2.8235	2.8462	3.0725	3.8022	3.8107
Maximum ΔE	12.8236	13.6256	13.6537	26.3483	27.6121	27.6055

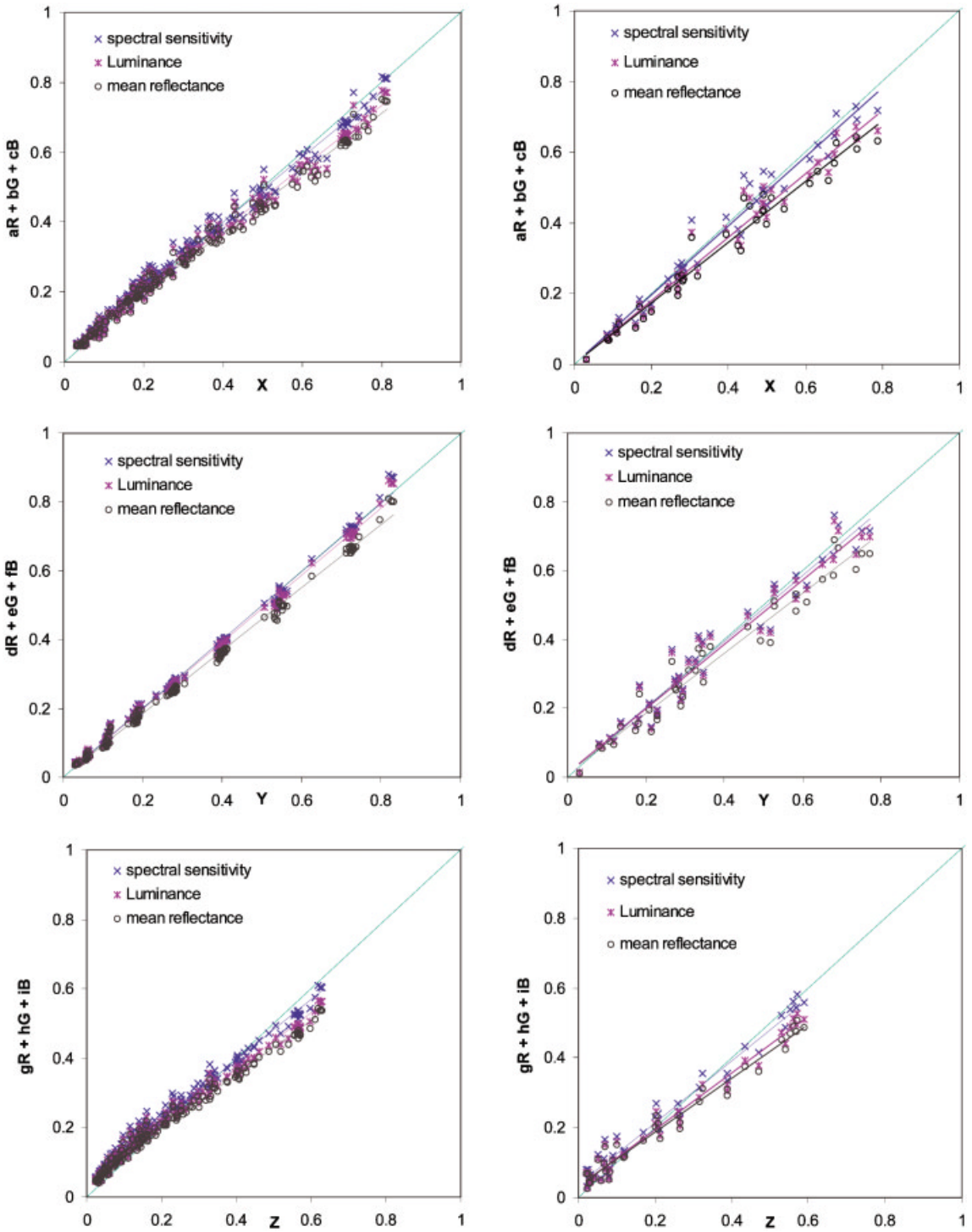

FIG. 4. Correlations for the DC samples (left) and the NCS samples (right) between tristimulus values and linear transforms of camera responses using different linearization techniques. The solid lines show linear regression fits and the dashed shows perfect linearization with a gradient of 1.

thors[21] have reported better characterization performance for the green channel than for the other two channels.

For the NCS samples, however, the difference between the spectral-sensitivities-based technique and the luminance-based technique is even more marked. Even for the *Y* tristimulus values (middle right in Fig. 4) the luminance-based technique performs poorly. It seems therefore that the luminance- and mean-reflectance-based techniques do not lead to proper linearization of the channel outputs and indirect but compelling evidence for this is provided in the characterization results shown in Table II.

DISCUSSION

This study investigated techniques for accounting for the nonlinearity of the input-output response of a camera sys-

TABLE IV. Correlation coefficients r for the data shown in Fig. 4.

	DC samples			NCS samples		
	Spectral sensitivities	Luminance	Mean reflectance	Spectral sensitivities	Luminance	Mean reflectance
X values	0.9964	0.9848	0.9837	0.9843	0.9782	0.9712
Y values	0.9986	0.9981	0.9879	0.9842	0.9823	0.9792
Z values	0.9865	0.9848	0.9761	0.9836	0.9803	0.9735

tem. A simple power-law form of the nonlinearity was assumed and estimates of the value for the exponent for each of the color channels were made using three different methods. Two of the three methods were based upon the relationship between the camera outputs and the Luminance or mean reflectance for a set of chromatically neutral Munsell patches. The third method used estimates of the spectral sensitivities of the camera channels to compute raw channel inputs for each of the Munsell samples. Linearization was carried out for an Agfa StudioCam camera and then characterization was carried out using the Macbeth ColorChecker DC samples and the performance of the characterization was tested using the Natural Color System samples. The results showed that characterization errors were up to 10% better using the spectral-sensitivities-based method than using the other two methods. A similar finding was reported in a previous study using simulated camera systems to compare these methods for linearization.[10] We therefore suggest that the spectral-sensitivities-based method is worth further consideration for characterization or any other computational process that requires linearization of the camera responses. We note, however, that the spectral-sensitivities-based method is a multistep method, whereas the other two methods are single-step methods. Further justification of the spectral-sensitivities-based method should compare its performance to multistep methods that do not incorporate the spectral sensitivities of the channels.

Finally, the advantages of the spectral-sensitivities-based method were apparent even though the camera that we used for this study was a "high-end" camera where the nonlinearity of the input/output response was quite small and where we used a crude (but relatively simple) method to estimate the spectral sensitivities. We expect greater benefits using this method for "low-end" camera systems and/or for cameras where the spectral sensitivities are known or more precisely estimated. We also expect the smoothness of the illumination to influence the error in the estimates of the nonlinearity using the luminance- and mean-reflectance-based methods.

1. Farrell JE, Sherman D, Wandell BA. How to turn your scanner into a colorimeter. In: Proceedings of the 10th International Conference on Advances in Non-impact Printing Technologies, Springfield, USA; 1994. p 579–581.
2. Wu W, Allebach JP, Analoui M. Imaging colorimetry using a digital camera. J Imag Sci Technol 2000;44:267–279.
3. Hong G, Luo MR, Rhodes PA. A study of digital camera colorimetric characterization based on polynomial modeling. Color Res Appl 2001;26:76–84.
4. Johnson T. Methods for characterizing color scanners and digital cameras. In: Green P, MacDonald LW, editors. Color engineering, achieving device independent color. New York: John Wiley & Sons; 2002.
5. Green P. Overview of characterization methods. In: Green P, MacDonald LW, editors. Color engineering, achieving device independent color. New York: John Wiley & Sons; 2002.
6. Johnson T. Methods for characterizing color scanners and digital cameras. Displays 1996;16:183–191.
7. Sun Q, Fairchild MD. Statistical characterization of spectral reflectances in human portraiture. In: Proceedings of the 9th Color Imaging Conference, Scottsdale, USA; 2001. p 73–79.
8. Thomson MGA, Westland S. Color-imager characterization by parametric fitting of sensor responses. Color Res Appl 2001;26:442–449.
9. Barnard K, Funt B. Camera characterization for color research. Color Res Appl 2002;27:152–163.
10. Cheung TLV, Westland S. Accurate estimation of the non-linearity of input-output response for color digital cameras. In: Proceedings of the Digital Photography Conference, Rochester, USA; 2003. p 366–369.
11. Connah D, Westland S Thomson MGA. Recovering spectral information using digital camera systems. J Colorat Technol 2001;117:309–312.
12. Frieden BR. Probability, statistical optics and data testing. Berlin: Springer-Verlag; 1983.
13. De La Maza M, Yuret D. Dynamic hill climbing. AI Expert 1994;9:26–31.
14. Finlayson GD, Hordley SD, Hubel PM. Recovering device sensitivities with quadratic programming. In: Proceedings of the 6th Color Imaging Science Conference, Scottsdale, USA; 1998. p 90–95.
15. Hubel PM, Sherman D, Farrell JE. A comparison of methods of sensor spectral sensitivity estimation. In: Proceedings of the 2nd Color Imaging Science Conference, Scottsdale, USA; 1994. p 45–48.
16. Hardeberg JY. Acquisition and reproduction of color images: colorimetric and multispectral approaches [PhD thesis]. Ecole Nationale Superieure des Telecommunications (France); 1999.
17. Cheung V, Westland S, Connah D, Ripamonti C. A comparative study of the characterisation of color cameras by means of neural networks and polynomial transforms. J Colorat Technol 2004;120:19–25.
18. Westland S, Ripamonti C. Characterization of cameras. In: Computational color science: Using MATLAB. Chichester, UK: John Wiley & Sons; 2004.
19. Borse GJ. Numerical methods with MATLAB: A resource for scientists and engineers. London, UK: PWS; 1997.
20. Erricker BC. Correlation. In: Advanced general statistics. London: The English Universities Press; 1971.
21. MacDonald LW, Ji W. Color characterization of a high-resolution digital camera. In: Proceedings of the 1st European Conference on Color in Graphics, Image and Vision, Poitiers, France; 2002. p 433–437.